Hydrogen Bonding of Ammonia with (H,OH)-Si(001) Revealed by Experimental and Ab Initio Photoelectron Spectroscopy

Lucía Pérez Ramírez, Jean-Jacques Gallet, Fabrice Bournel, Florence Lim, Stéphane Carniato, François Rochet, Oleg Yazyev, Alfredo Pasquarello, Elena Magnano, Federica Bondino

Hydrogen Bonding of Ammonia with (H,OH)-Si(001) Revealed by Experimental and *ab initio* Photoelectron Spectroscopy

Lucía Pérez Ramírez[1], Jean-Jacques Gallet[1,2], Fabrice Bournel[1,2], Florence Lim[1], Stéphane Carniato[1], François Rochet[1]*, Oleg V. Yazyev[3], Alfredo Pasquarello[3], Elena Magnano[4,5] and Federica Bondino[4]*

[1] Sorbonne Université, CNRS, Laboratoire de Chimie Physique matière et Rayonnement, UMR 7614, 4 place Jussieu, 75005 Paris, France

[2] Synchrotron SOLEIL, L'Orme des Merisiers, Saint-Aubin - BP 4891192 Gif-sur-Yvette CEDEX, France

[3] Chaire de Simulation à l'Echelle Atomique (CSEA), Ecole Polytechnique Fédérale de Lausanne (EPFL), CH-1015 Lausanne, Switzerland

[4] IOM-CNR, Laboratorio TASC, 34149 Basovizza, Trieste, Italy

[5] Department of Physics, University of Johannesburg, PO Box 524, Auckland Park 2006, South Africa

ABSTRACT. Combining experimental and *ab initio* core-level photoelectron spectroscopy (periodic DFT and quantum chemistry calculations), we elucidated how ammonia molecules bond to the hydroxyls of the (H,OH)-Si(001) model surface at a temperature of 130 K. Indeed theory evaluated the magnitude and direction of the N 1s (and O 1s) chemical shifts, according to the nature (acceptor or donor) of the hydrogen bond, and, when confronted to experiment, showed unambiguously that the probe molecule makes one acceptor and one donor bond with a pair of hydroxyls. The consistency of our approach was proved by the fact that the identified adsorption geometries are precisely those that have the largest binding strength to the surface, as calculated by periodic DFT. Real-time core-level photoemission enabled the measurement of the adsorption kinetics of H-bonded ammonia and its maximum coverage (0.37 ML) under 1.5×10^{-9} mbar. Experimental desorption free energies were compared to the magnitude of the adsorption energies provided by periodic DFT calculations. Minority species were also detected on the surface. As in the case of H-bonded ammonia, DFT core-level calculations were instrumental to attribute these minority species to datively bonded ammonia molecules, associated to isolated dangling bonds remaining on the surface, and to dissociated ammonia molecules, resulting largely from beam damage.

1. Introduction

Hydrogen bonding, that combines directionality and strength[1] is common in nature (in water chemistry, biochemistry and mineralogy), and is also harnessed to produce supramolecular scaffolds.[2] As a special case of supramolecular chemistry, adsorbates H-bonded on hydroxyl-covered surfaces, especially technologically relevant oxides like titania, has aroused considerable

interest, due to their implication in electrochemistry, (photo-)catalysis etc..[3] However, surface science studies that addressed the issue of H-bonding using core level x-ray photoelectron spectroscopy (XPS) are relatively scarce, in comparison with vibrational spectroscopies that occupy the central stage.[4,5] In particular, the impact of hydrogen-bonding on core-level shifts, which can be large as we shall see in the following, has not been enough rationalized, to the point that it has been sometimes misinterpreted, e.g. as due to a proton transfer in the case of amines deposited on hydroxylated surfaces.[6,7,8]

In a context where XPS really needs the support of *theoretical* methods to interpret the experimental spectra, the seminal theoretical paper by Felicíssimo et al. (2005) may not have gotten the attention that it deserved.[9] Addressing a simple system, the H_2O dimer, these authors, who used the *ab initio* complete active space self-consistent (CASSCF) method, calculated that the O 1s ionization energy was split into two components separated by 1.29 eV due to intermolecular H-bonding. The H-accepting O 1s level is pushed to higher ionization energy, while the H-donating O 1s level is shifted to lower ionization energy. Subsequent density functional theory (DFT) calculations by some of us then led to similar results, with an O 1s energy splitting of 1.7 eV.[10] A more recent theoretical work, carried out to calculate O 1s and N 1s core level shifts in H bonded organic molecules,[11] confirmed the trends on the direction of the chemical shifts and scaled their magnitude with the H-bond lengths. Concerning surfaces, the combined theoretical and experimental effort was devoted to the anatase TiO_2 surface, as an attempt to resolve the question of water adsorption and dissociation on its (101) face.[12,13] However, at the experimental level, the detailed measurements of binding energy shifts on titania surfaces, in particular the effect on the hydroxide O 1s core-levels of the adsorbates, (see Ref. [12]) is hampered by the strong contribution of bulk oxygen in the O 1s spectrum. Therefore, the

simplest case study for testing the effectiveness of combined *ab initio* and experimental core-level spectroscopy in tackling the H-bond issue would consider a simple and well-described hydroxyl surface exposed to a molecule like ammonia or an amine, to eliminate "interferences" in the analysis of the core-levels.

To meet these specifications, we have chosen the water-terminated Si(001)-2×1 surface,[10,14,15,16,17,18,19,20,21] denoted (H,OH)-Si(001) in the following. In addition to being a model system, the presence of OHs makes this surface the ideal substrate for the growth of high *k* dielectric oxides *without SiO_2 interlayer* via atomic layer deposition (ALD),[22,23,24,25] and enables molecular grafting via an esterification reaction with carboxylic heads.[26,27] (H,OH)-Si(001) results from the exposure of the clean dimerized Si(001) 2x1 surface to water vapor at room temperature in ultra-high vacuum conditions. The dissociative reaction of water with the silicon dimers leads to the formation of half a monolayer (ML) of SiH and half a monolayer of SiOH (one ML corresponds to 6.8×10^{14} atoms/cm^2). One key feature of the reacted surface is the fact that the silicon dimer bond remains intact when the exposure is made at room temperature,[28,15] as the oxygen insertion process in dimer bonds or in back bonds is only effective at a higher temperature, as shown by scanning tunneling microscopy (STM).[20] The spatial arrangements of silicon monohydrides and hydroxyls is now well known, thanks to STM.[14,18,19,20] They are schematically depicted in Figure 1. The hydroxyls are found aligned along the same side of the dimer row, in *striped patterns* (SP), or alternately, they can form *checkerboard patterns* (CBP). Due to the competition between on-dimer and intra-row (inter-dimer) dissociation paths,[29–31] two OH (and conversely two H) can also sit on the same dimer (ODIM paired OHs). On average this occurs every five to six dimers in a row.[18] A further consequence of the competition between on-dimer and intra-row dissociation channels, is the fact that about a few hundredths of a ML

(~4.0±0.4×10^{-2} ML on n^+ doped Si(001)[19]) of tri-coordinated silicon atoms (the so-called isolated dangling bonds or IDB) are left[14,18,19,20,21] even after prolonged exposures to water at room temperature. These electrically active defects are responsible for fixing the Fermi level in the silicon surface gap. [19,21] When the H-bond pairing of surface hydroxides is of concern, or the H-bonding of probe molecules with the latter ones, both the distance between OHs and their topological distribution matter. In this respect, (H,OH)-Si(001) has clear advantages over hydroxylated vitreous/amorphous silica surfaces for which the OH coverage and bonding is highly dependent on the history of the material. For (H,OH)-Si(001), the striped (SP) or checkerboard (CBP) patterns, can be theoretically modeled by periodic calculations in a way that is not too expensive in terms of cell size,[17] and questions related to the realism[32] of modeling hydrated amorphous SiO_2 surfaces can be removed.

The present article explicitly discusses hydrogen bonding between ammonia and the hydroxyls of the (H,OH)-Si(001) surface and its effects on the N 1s and O 1s core-levels of the adsorbate and surface, respectively. *Real-time, in-situ* synchrotron radiation x-ray photoelectron spectroscopy (XPS) was implemented while (H,OH)-Si(001) was exposed to NH_3 under 5×10^{-9} mbar at a temperature of 130 K. The support of DFT calculations was essential to interpret the observed core-level binding energy shifts. Using a periodic slab density functional theory (DFT) approach, molecular dynamics were undertaken with the Car-Parinello approach. Then the adsorption energies of representative geometries were calculated, as well as their relative photoemission binding energies. In addition to the periodic approach, the core-level ionization energies were calculated using a cluster-type quantum chemistry (QC) DFT approach. A useful comparison can be made between the two different theoretical approaches, and between theory as a whole and experiments.

The major output of the present paper is the clear-cut demonstration that the XPS N 1s core-level binding energies are highly sensitive to the formation of H-bonds, and more specifically to their acceptor or donor nature that leads to shifts in opposite directions. The "algebraic additivity" of core-level shifts is emphasized by *ab initio* DFT spectroscopy, which enables theory to make the "reverse engineering"[12] of multiple H-bonding. In particular, core-level spectroscopy highlights the formation of double hydrogen bonds for ammonia (acceptor and donor). This new spectroscopic insight of the complex H-bonding of ammonia with surface OHs may be of practical interest, especially in the context of ALD, where ammonia, or an amine, is used as a catalyst.[33–35,36,37]

Finally, besides the majority H-bonded ammonia species, XPS has also identified side reactions leading to minority species *chemisorbed* on the surface, i.e. dissociated ammonia molecules (due in part to synchrotron beam damage) and ammonia molecules *datively-bonded* to the isolated dangling bonds. The latter observation is interesting, as it is closely related to the use of H-terminated silicon as a gas sensor,[38] or to the molecular doping of meso- and nano-structured silicon.[39,40]

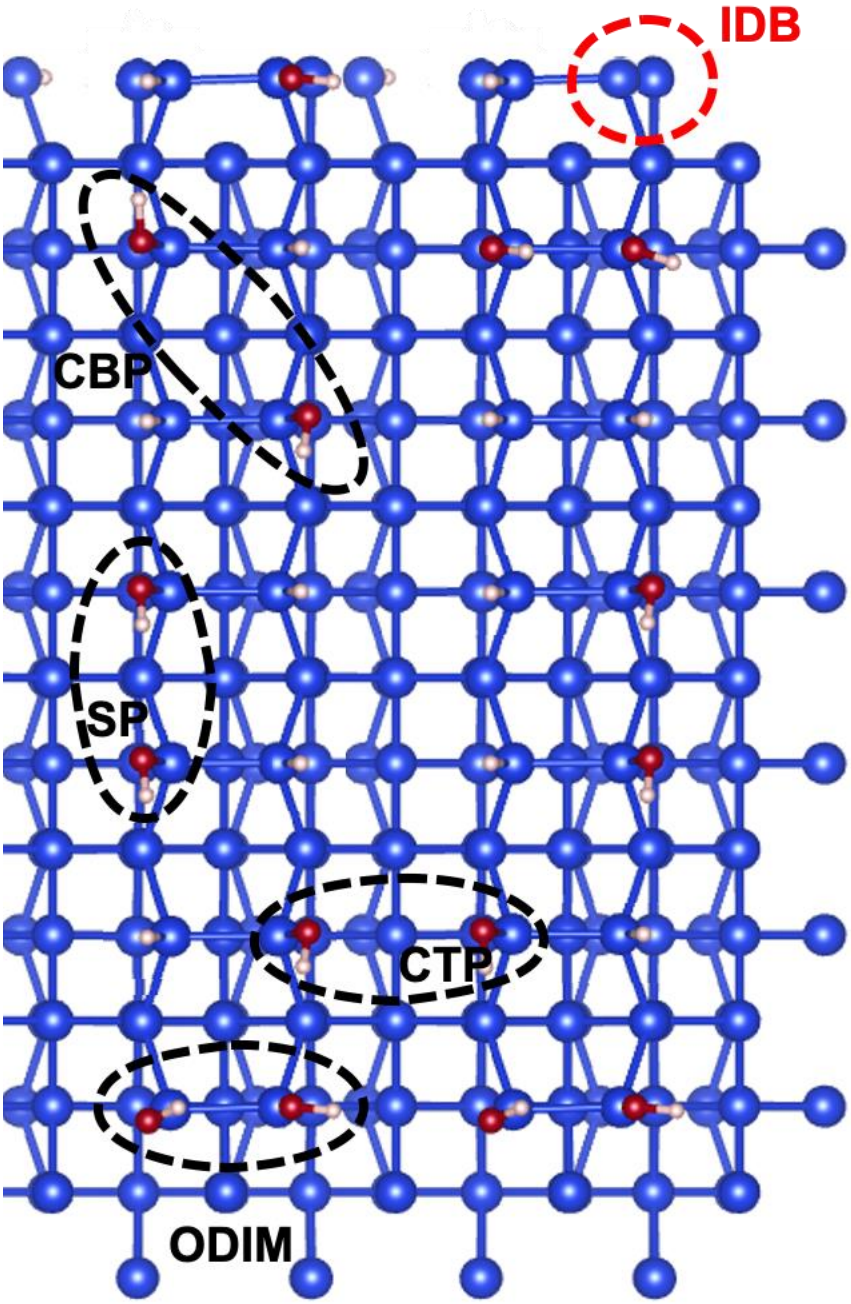

Figure 1. Ball and stick views of (H,OH)-Si(001). Silicon, oxygen and hydrogen atoms are in blue, red and white, respectively. The OHs can form checkerboard patterns (CBP) and striped patterns (SP). On dimer (ODIM) and "cross-trench pattern" (CTP) OH pairs are also shown. Tri-

coordinated silicon atoms, bearing an "isolated dangling bond" (IDB), are also depicted (their surface coverage amounts to ~4×10^{-2} ML).

2. Methods

2.1. Surface preparation.

The surface preparation was described in detail in our preceding publications.[10,27,41] We used a heavily phosphorus doped silicon wafer (n^+) of resistivity 0.003 Ω.m. After surface cleaning by Joule heating, the clean reconstructed Si(001)-2×1 surface is exposed to H_2O vapor at room temperature for 15 min under a pressure of 5×10^{-9} mbar. Under these conditions the surface is saturated by water (see below).[21] Then the surface was cooled down to 130 K and exposed to NH_3 gas.

2.2. Synchrotron radiation XPS at BACH beamline

Electron spectroscopy measurements were performed at BACH Beamline, ELETTRA synchrotron facility (Trieste, Italy). Linearly polarized light in the 175-600 eV range is provided by a high energy APPLE II helical undulator. The photon dispersion system is based on a Padmore variable angle spherical grating monochromator. Photoemission spectra were measured by means of a modified 150 mm VSW hemispherical electron analyzer with a 16-channel detector. In the adopted geometry, the photon beam direction was perpendicular to the sample surface (the polarization was contained in the surface plane) and the photoelectron emission angle was at 60° from the sample surface.

The N 1s and O 1s spectra were measured at 455 eV and 595 eV, respectively. The spectra, after Shirley background subtraction, are fitted with sums of Gaussians. The Si 2p core level spectrum of (H,OH)-Si(001), measured at $h\nu$=175 eV, and shown in Figure S1, section S1 of the supporting information (SI), indicates that the surface is saturated by water fragments H and OH. The few isolated dangling bonds remaining on the surface (~$4.0\pm0.4\times10^{-2}$ ML) are doubly occupied and hence negatively charged.[21] The bulk Si $2p_{3/2}$ binding energy is measured at 99.41 eV at 300 K. After cooling down to 130 K, the Si 2p spectrum moves slightly to higher binding energy, because of a surface photovoltage effect that decreases the upward band bending at the surface. Therefore, all spectra acquired at low temperature (N 1s and O 1s) are corrected for this shift, keeping the Si $2p_{3/2}$ position at 99.41 eV.

2.3. DFT slab periodic calculations

The periodic DFT calculations utilize plane waves in conjonction with norm-conserving and ultrasoft (for N and O) pseudopotentials. We used a cutoff of 35 Ry for the electron wave functions and of 280 Ry for the electron density. The calculations have been carried out using the CPMD code.[42] The exchange correlation is described through the semi-local functional proposed by Perdew, Becke and Ernzerhof (PBE).[43] The model consists of a silicon slab of 6 layers with a $\sqrt{8} \times \sqrt{8}$ surface repeat unit resulting in a total number of 48 Si atoms. The Si lattice parameter (5.49 Å) corresponds to the lattice constant of bulk Si equilibrated at the PBE level. The Brillouin zone of the simulation cell is sampled at the Γ point only. The Si dangling bonds of the bottom layer are saturated with H atoms. The slabs are separated by 10 Å, which ensures that the images do not produce any effect on the result.

In this study, we also performed Car-Parrinello molecular dynamics[44] to explore possible bonding configurations. We used a fictitious mass of 400 a.u., a time-step of 0.12 fs. The temperature was controlled by a Nosé-Hoover thermostat and was set to 150 K. The adsorbates were allowed to evolve freely, and the structures obtained were monitored. In the different molecular dynamics simulation runs, we considered 1, 3 and 5 NH_3 molecules per supercell. The molecular dynamics simulations globally lasted up to 14 ps. The adsorption energies (E_{ads}) per molecule are total energy differences. They do not take into account any entropic effects nor any zero-point energy contributions.

For the core-level shifts (CLS_{per}^{th}), a modified N pseudopotential was constructed corresponding to a N atom with a hole in the 1s shell. The method is similar to the one used in a series of papers by Rignanese and Pasquarello.[45,46] We considered various adsorbates configurations fully relaxed to equilibrium.

2.4. Cluster quantum chemistry (QC) DFT calculation of N 1s core ionization potentials

We follow here a well-proven approach to calculate the excitation energies of the atomic core levels of adsorbates on silicon.[10,47] The calculation procedure, making use of the GAMESS (US)[48] software, is the same as that described in detail in previous studies. The clean silicon substrate is mimicked by a "one-dimer cluster" containing nine silicon atoms and 12 termination hydrogens (Si_9H_{12}), a "two-dimer-in-a-row" cluster containing 15 silicon atoms and 16 termination hydrogens ($Si_{15}H_{16}$), or a "three-dimer-in-a-row" cluster containing 21 silicon atoms and 20 termination hydrogens ($Si_{21}H_{20}$). The bare dimer is decorated by the appropriated fragments (H,OH), (OH,OH) and (H,NH_2). The ammonia molecule is then H-bonded to the hydroxyls in the striped pattern (SP), checkerboard pattern (CBP) and on-dimer (ODIM) paired

OHs sites. A bare dimer can also accept a NH_3 molecule that makes a dative bonding with one silicon dangling bond.

Ground-state optimized geometries have been optimized calculated using the Becke3 Lee-Yang-Parr (B3LYP) functional and effective core potentials (SBKJ + d polarization) for the substrate silicon atoms, using a 6-311G+* basis sets for carbon, nitrogen and oxygen including polarization (*) and diffuse functions (+), and 6-31G* for hydrogen. Theoretical N 1s or O 1s ionization energies (ΔIE_{QC}^{th}) were calculated as the energy difference between the core-ionized and the ground state within the ΔKohn-Sham approach and where the 6-311G+* basis set is substituted by the IGLOO III basis set on the core-hole site.

Relativistic corrections (0.3 eV for N 1s and 0.4 eV for O 1s) are included in the calculation. The N 1s IE_{QC}^{th}values (405.7 eV for NH_3) are found within ±0.1 eV of the measured ones,[49] which is a good validation test for the method.

The question of the energy reference requires a comment. In cluster QC calculations, the IE^{th} reference energy is the vacuum level at infinity VL^{∞}, where the electron has zero energy. Therefore, the N 1s or O 1s IE^{th} is that of a "gas phase molecule" consisting in the surface-mimicking cluster plus ammonia. However, in XPS studies of a solid, the energy reference of ionization energies (called in this case binding energies, BE) is the Fermi level energy, FL (common to the sample and spectrometer). Unfortunately, VL^{∞} is inaccessible to measurement, and hence no common reference exists between XPS and cluster calculations. What is measurable is the work function WF that is by definition $WF = VL_{av}^{surf} - FL$, the difference between the energy position of the vacuum level "immediately" out of the solid surface VL_{av}^{surf} (a surface-cell averaged value that depends on the surface dipole electrostatic potential), and FL.

Considering different adsorption geometries also forces us to consider different local work functions on the surface. With a local vacuum level $\mathrm{VL}_{\mathrm{loc}}^{\mathrm{surf}}$, we can define as well a local work function, $\mathrm{WF}_{\mathrm{loc}} = \mathrm{VL}_{\mathrm{loc}}^{\mathrm{surf}} - \mathrm{FL}$ (FL is considered not to vary over the surface). *We pin the* IE_{QC}^{th} *to the local vacuum level.* The same concept is used in photoelectron spectroscopy of adsorbed xenon.[50] Then the IE_{QC}^{th} of the configuration of interest is related to the binding energy BE (referenced to FL) by the following equation:

$$\mathrm{IE}_{QC}^{th} = \mathrm{BE} + \mathrm{WF}_{\mathrm{loc}} \quad [1]$$

When we compare two different adsorption geometries, we calculate their difference in IE_{QC}^{th}. One gets:

$$\Delta\mathrm{IE}_{QC}^{th} = \Delta\mathrm{BE} + \Delta\mathrm{WF}_{\mathrm{loc}} \quad [2]$$

Therefore $\Delta\mathrm{IE}_{QC}^{th} = \Delta\mathrm{BE}$ *only* when $\Delta\mathrm{WF}_{\mathrm{loc}}$ is negligible in equation [2]. This *caveat* should always be kept in mind. In the following, the reference species for N 1s $\Delta\mathrm{IE}_{QC}^{th}$ will be the amine ($\mathrm{HSi\text{-}SiNH_2}$). For the O 1s $\Delta\mathrm{IE}_{QC}^{th}$ the isolated hydroxyl, see SI, section S3.

3. Results and discussion

3.1 DFT simulations of adsorption geometries and core-level binding energy shifts

Periodic DFT calculations. The ammonia molecule was placed at SP, CBP and CTP sites indicated in Figure 1 (the ODIM paired OHs site was not examined). Here and in the following, we adopt a systematic nomenclature to identify hydroxyls and ammonia molecules accepting

(denoted A or a) or donating (denoted D or d) a hydrogen atom. Capital letters mean that the H-bond is strong (H-bond length below 2.2 Å). Lower case letters are used when the H-bond is considered weak (H-bond length greater than 2.2 Å).

After Car-Parrinello molecular dynamics, the initial SP-NH_3(A,D) and (A,A) configurations were preserved. However, initial CBP-NH_3(A,D), (D,D) and (A,A) configurations ended up as CBP-NH_3(A,d), CBP-NH_3(d,d) and CBP-NH_3(A,d). Initial CTP-NH_3(A,D), (D,D) and (A,A) configurations all ended up as CTP-NH_3(A,d). Mininum energy geometries in SP and CBP sites are shown in Figure 2.

The negative of the adsorption energies $-E_{ads}$ obtained from structural relaxation in the periodic DFT set-up (corresponding to T=0 K) are given in Table 1, together with the N 1s core-level shift relative to that of the H-Si-Si-NH_2 moiety, CLS_{per}^{th}. The Si-NH_2 fragment is used as a benchmark of the XPS binding energies, because it is well documented.[47] The most stable configurations ($-E_{ads} > 0.56$ eV) are the SP-NH_3(A,D), the CBP-NH_3(A,d), and the cross-trench pattern (CTP) NH_3(A,d). All these configurations have a CLS_{per}^{th} in the range 1.41 to 1.51 eV (see Table 1).

The other adsorption geometries have $-E_{ads}$ values significantly smaller than that of the acceptor-donor ones. The SP NH_3(A,A) geometry has an $-E_{ads}$ value of 0.42 eV, and thus is less strongly attached to the OH pairs than the (A,D) or (A,d) geometries. Its calculated CLS_{per}^{th} of 2.2 eV with respect to the dissociated H-Si-Si-NH_2 configuration is also noticeably greater than that of the acceptor/donor geometries by about +0.8 eV. Molecules adopting the NH_3(d,d) geometries are still more weakly bound to the surface with $-E_{ads}$ equal to 0.18 eV (SP) and 0.03 eV (CBP). Their calculated N 1s binding energy difference is small (less than 0.2

eV) with respect to that of Si-NH_2. Finally, from a spectroscopic viewpoint, the fact that the mixed NH_3(A,D) or NH_3(A,d) adsorption geometries lead to N 1s binding energies intermediate between that of NH_3(d,d) and that of NH_3(A,A) is consistent. In fact, acceptor bonding shifts the N 1s binding energy to higher values while donor bonding counterweights this effect**.**

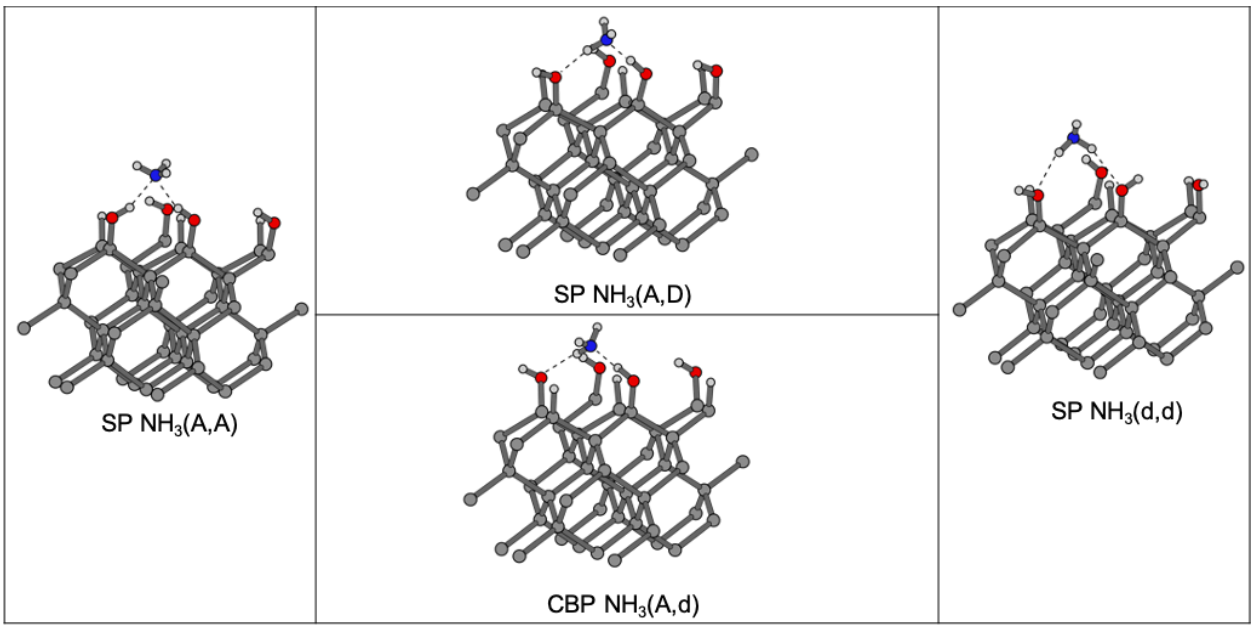

Figure 2. NH_3/OH equilibrium geometries calculated via the periodic DFT approach: silicon, oxygen, nitrogen, and hydrogen atoms are in grey, red, blue, and white, respectively. Nomenclature: striped pattern (SP), checkerboard pattern (CBP). A is for strong acceptor; D (d) is for strong (weak) donor (see text). We give in Table 1 the adsorption energies of structurally relaxed molecules (E_{ads}) (calculated at 0 K) and their corresponding binding energy shifts (CLS^{th}_{per}), as obtained by the periodic DFT approach. The most strongly bonded geometries are of the type NH_3(A,D) or NH_3(A,d) type. These are the ones observed experimentally (see text).

Periodic DFT			
configuration	H bond lengths (Å)	$-E_{ads}$ (eV)	CLS_{per}^{th} N 1s core level shift with respect to Si-NH_2 (eV)
H-Si-Si-NH_2	NA	3.29	0
NH_3-Si-Si	NA	2.38	3.02
SP NH_3(A,D)	A: 1.64 D: 2.00	0.69	1.41
CBP NH_3(A,d)	A: 1.74 d: 2.45	0.61	1.44
CTP NH_3(A,d)	A: 1.67 d: 2.56	0.56	1.51
SP NH_3(A,A)	A: 2.00 A: 2.01	0.42	2.2
CBP NH_3(d,d)	d: 2.46 d: 2.49	0.18	0.29
SP NH_3(d,d)	d: 2.36 d: 2.47	0.06	0.15

Table 1. Periodic DFT geometries, adsorption energies (E_{ads})) and N 1s binding energy core-level shifts (CLS_{per}^{th}) with respect to Si-NH_2 for structurally relaxed configurations (at 0 K). Nomenclature: striped pattern (SP), checkerboard pattern (CBP), and cross-trench (CTP). The

configurations are listed (from top to bottom) according to decreasing $-E_{ads}$ i.e. decreasing binding strength. A capital letter corresponds to a strong H bond, a lower case to a weak H bond (a H bond is considered weak when its length is longer than 2.2 Å).

Cluster QC DFT calculations. For their part, the cluster QC DFT calculations have addressed ammonia bonding on SP and CBP patterns mimicking those of the periodic DFT calculations. We have also considered ammonia bonded on ODIM OHs pairs. Some optimized geometries are shown in Figure 3.

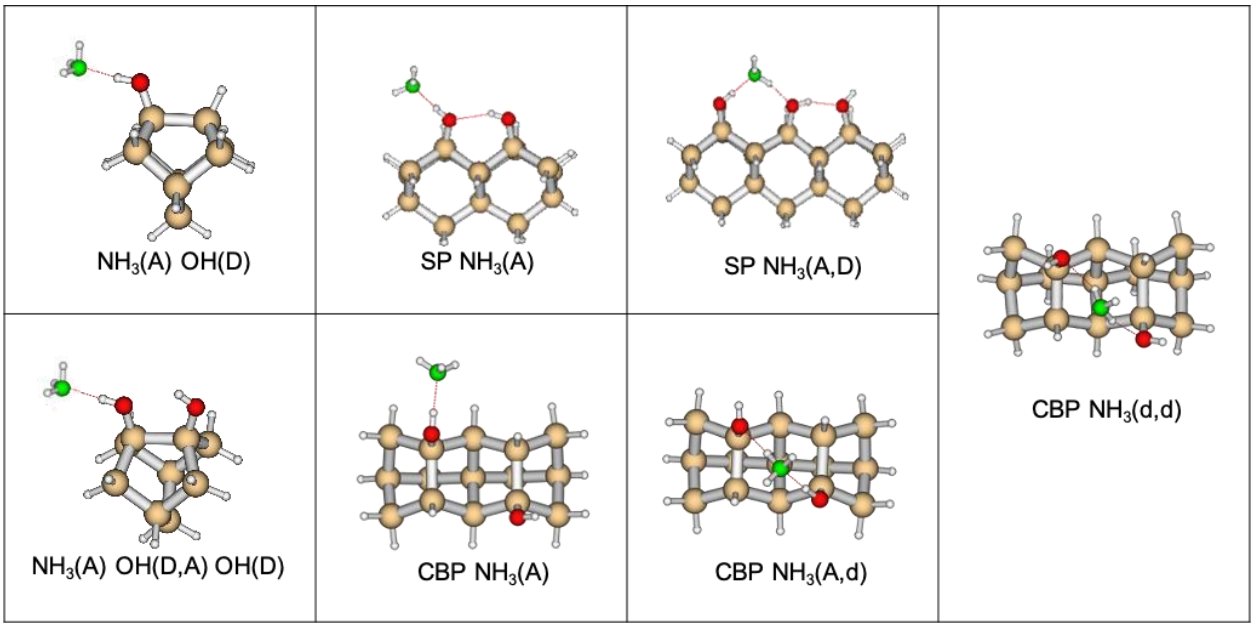

Figure 3. NH_3/OH equilibrium geometries calculated via the cluster QC DFT approach: silicon, oxygen, nitrogen, and hydrogen atoms are in brown, red, green, and white, respectively. The

nomenclature is the same as in Figure 2 (see also text). The O 1s and N 1s calculated ionization potentials (IE_{QC}^{th}) of the cluster are given in Table 2.

Absolute N 1s IE_{QC}^{th} are reported in Table 2. First it is convenient to compare the IE_{QC}^{th} of the various configurations with that of gas phase ammonia (405.7 eV). All purely acceptor geometries have IE_{QC}^{th} higher by ~0.7 eV than the isolated molecule. In contrast, all purely donor geometries have IE_{QC}^{th} lower than that of isolated ammonia by ~1.1 eV. Dual acceptor/donor geometries have IE_{QC}^{th} nearly equal to that of isolated ammonia. This observation strongly suggests the electrostatic origin of the changes in IE_{QC}^{th} for the molecule, the presence of protons rising the ionization energy and that of the electron lone pair decreasing it. Acceptor/donor bonds result in a quasi-cancellation of these opposite effects. The same trends were observed in periodic DFT.

To enable a comparison with the periodic DFT core-level shifts CLS_{per}^{th}, we calculate the ΔIE_{QC}^{th} values referenced to dissociated ammonia ($SiNH_2$). The IE_{QC}^{th} of $SiNH_2$ is 404.0 eV for a Si_9H_{12} (NH_2,H) cluster, a value identical to that found for a CBP $Si_{15}H_{16}$ (2H,2NH_2) cluster (Figure 1 in Ref. [47]). Purely acceptor bonds have ΔIE_{QC}^{th} in the 2.3-2.5 eV range. NH_3(A) geometries with a *single* H-bond of 1.84±0.02 Å have practically the same IE_{QC}^{th} of a double H-bond SP-NH_3(A,A) geometry with two longer H-bonds, of 2.05±0.03 Å. The QC calculation ΔIE_{QC}^{th} are in close agreement with the CLS_{per}^{th} of SP-NH_3(A,A), equal to 2.2 eV. The SP-NH_3(A,D) and CBP-NH_3(A,D) have both the same ΔIE_{QC}^{th} equal to 1.48 eV. The ΔIE_{QC}^{th} of the ODIM NH_3(A,D) configuration is somewhat larger, 1.68 eV, because of the shorter A

bond (1.77 Å). Again the ΔIE_{QC}^{th} values are remarkably close to the CLS_{per}^{th} found for the corresponding geometries (1.41-1.44 eV, Table 1). Considering the donor geometries, ΔIE_{QC}^{th} is in the 0.48-0.76 eV range. If we consider specifically the CBP-NH_3(d,d) configuration, the most strongly adsorbed donor geometry according to periodic DFT, ΔIE_{QC}^{th} is 0.48 eV, close to the CLS_{per}^{th} of 0.29 eV for the same geometry.

Configuration	Cluster plus fragments or adsorbate	H-bond lengths (Å)	N 1s IE_{QC}^{th} (eV)	ΔIE_{QC}^{th} $SiNH_2$ reference (eV)
Free ammonia molecule NH_3		NA	405.70	
Benchmark adsorption geometries		NA		
Single dimer H-Si-Si-NH_2	Si_9H_{12} (NH_2,H)	NA	404.00	0
CBP H-Si-Si-NH_2	$Si_{15}H_{16}$ (2H,2NH_2)	NA	403.99	0
Si-Si-NH_3 datively bonded	$Si_{15}H_{16}$ (NH_3)	NA	406.98	2.99
H-bonding				
ODIM OH(d)... OH(a,D)…NH_3(A)	Si_9H_{12} (2OH,NH_3)	O-H...OH 2.64 O-H....NH_3 1.84	406.50	2.51
SP OH(D)... OH(A,D)…NH_3(A)	$Si_{15}H_{16}$ (2OH,2H,NH_3)	O-H...OH 2.15 O-H....NH_3 1.82	406.47	2.48
SP OH(D)... NH_3(A,A)…OH(D)	$Si_{15}H_{16}$ (2OH,2H,NH_3)	OH...NH_3 2.08 H_3N...HO 2.03	406.45	2.46
Single dimer OH(D)...NH_3(A)	Si_9H_{12} (OH,H,NH_3)	O-H…NH_3 1.84	406.38	2.39
CBP OH(D)…NH_3(A)	$Si_{15}H_{16}$ (2OH,2H,NH_3)	OH…NH_3 1.86	406.28	2.29
ODIM OH(D)…NH_3(A,D)…OH(A)	Si_9H_{12} (2OH,NH_3)	O-H...HNH_2 1.77 H_2NH....O-H 2.11	405.67	1.68
CBP OH(D)…NH_3(A,D)…OH(A)	$Si_{15}H_{16}$ (2OH,2H,NH_3)	OH…NH_3 1.82 H_2NH…OH 2.17	405.47	1.48
SP OH(D)…NH_3(A,D)…OH(A)	$Si_{21}H_{20}$ (3OH,3H,NH_3)	OH…NH_3 1.78 H_2NH…OH 2.04	405.47	1.48
Single dimer OH(A)...NH_3(D)	Si_9H_{12} (OH,H,NH_3)	H-O…H-NH_2 2.17	404.75	0.76
SP OH(d)…OH(a,D)...NH_3(D)	$Si_{15}H_{16}$ (2OH,2H,NH_3)	H-O…H-NH_2 2.14	404.56	0.57
CBP OH(a)…NH_3(d,d)…OH(a)	$Si_{15}H_{16}$ (2OH,2H,NH_3)	OH…HNH_2 2.35 H_2NH…OH(a) 2.35	404.47	0.48

Table 2. Theoretical N 1s ionization potential energies IE_{QC}^{th} calculated via a DFT QC silicon cluster approach. ΔIE_{QC}^{th} is the ionization energy referenced to that of the Si-NH_2 fragment. Si_9H_{12}, $Si_{15}H_{16}$ and $Si_{21}H_{20}$ are the "one-bare-dimer" , "two-bare-dimer-in-a-row" and "three-bare-dimer-in-a-row" clusters, respectively. (…) denotes a H-bond. We use the following nomenclature: on-dimer (ODIM), striped pattern (SP), checkerboard pattern (CBP). OH and NH_3 can donate (D or d) or accept (A or a) H atoms. A capital letter corresponds to a strong H bond, a lower case to a weak H bond (a H bond is considered weak when its length is longer than 2.2 Å).

3.2 Real-time core-level XPS

Identification of ammonia adsorbates. During *real-time* N 1s XPS measurements (at hν=455 eV), the exposure to NH_3 is made at 120 K by filling the analysis chamber up to a pressure of 5×10^{-9} mbar. Considering a gas temperature of 300 K, the flux *F* of molecules impinging on the surface is 1.85×10^{12} molecules cm^{-2} s^{-1}, equivalent to 2.72×10^{-3} ML s^{-1}, where one monolayer (ML) is the number of silicon atoms per unit surface (6.8×10^{14} cm^{-2}). The dose $Q=F\times t$ (where *t* is the exposure time) is expressed in ML in the following. After dosing for 865 s (Q=2.35 ML), the X-ray spot was displaced to probe another area, to check for possible beam-induced chemistry. Then after an overall exposure of 1150 s (Q=3.2 ML), ammonia was pumped down.

The question of co-adsorption of molecular water during cooling and then exposure to ammonia was examined by measuring the normalized O 1s intensity (see SI, section S2). The oxygen

coverage at room temperature is 0.50 ML, because almost all silicon atoms are covered by an equal number of H and OH. The surface sample at 130 K before ammonia exposure has an oxygen surface coverage of 0.57 ML (known with a precision of 8%). The increase may be attributed to water co-adsorption (see SI sections S3 and S4). However, after exposure to ammonia, we find an oxygen coverage of 0.50 ML again. Ammonia likely displaces the water molecules adsorbed on the surface. Therefore, we exclude the formation of NH_3/H_2O H-bonds, the probe molecule only binds to surface hydroxyls.

The time-resolved N 1s spectra (*each spectrum is the sum of 5 individual spectra)* is given in Figure 4(a). An illustrative N 1s spectra, with the corresponding fit by a sum of Gaussians, is given in Figure 4(b). The N 1s intensity is normalized with respect to the (H,NH_2)-Si(001) standard surface (N coverage of 0.5 ML), as shown in section S2 of the SI. In Figure 4(c), we plot against time the normalized coverages (in ML) of the various chemical components resulting from the fit of the N 1s spectra.

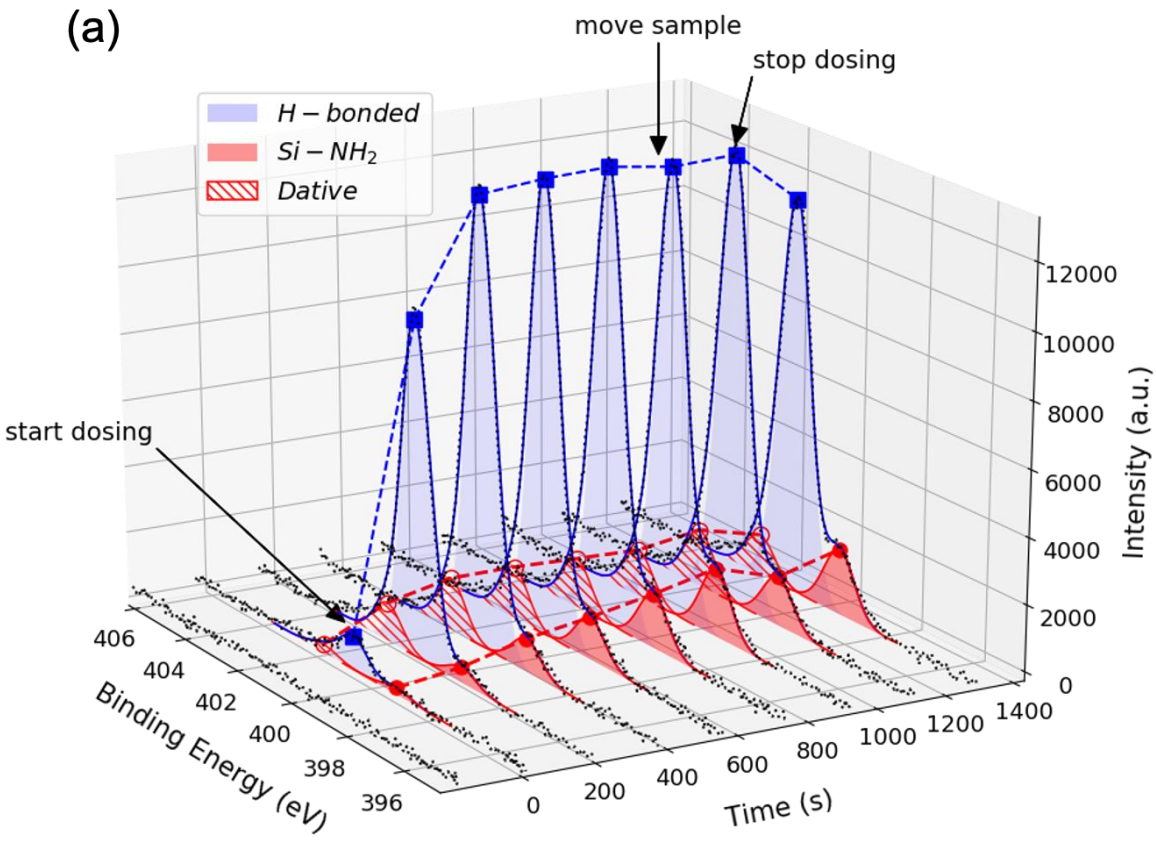
(a)
move sample
stop dosing
start dosing
H – bonded
Si – NH2
Dative
Intensity (a.u.)
12000
10000
8000
6000
4000
2000
0
406
404
402
400
398
396
Binding Energy (eV)
0
200
400
600
800
1000
1200
1400
Time (s)

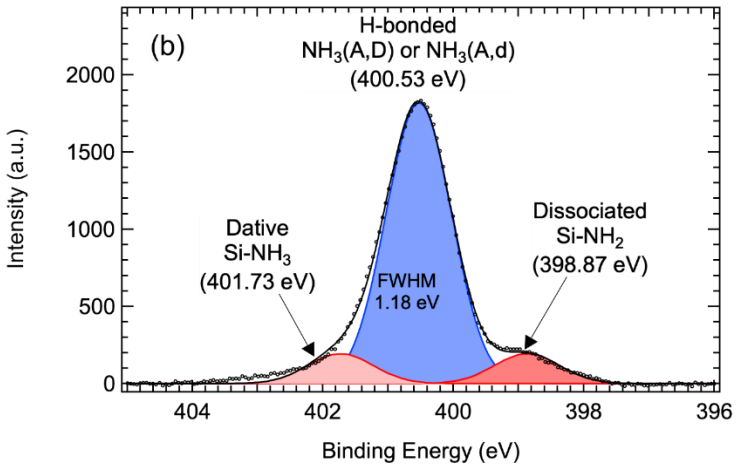
(b)
H-bonded
NH3(A,D) or NH3(A,d)
(400.53 eV)
Dative
Si-NH3
(401.73 eV)
FWHM
1.18 eV
Dissociated
Si-NH2
(398.87 eV)
Intensity (a.u.)
2000
1500
1000
500
0
404
402
400
398
396
Binding Energy (eV)

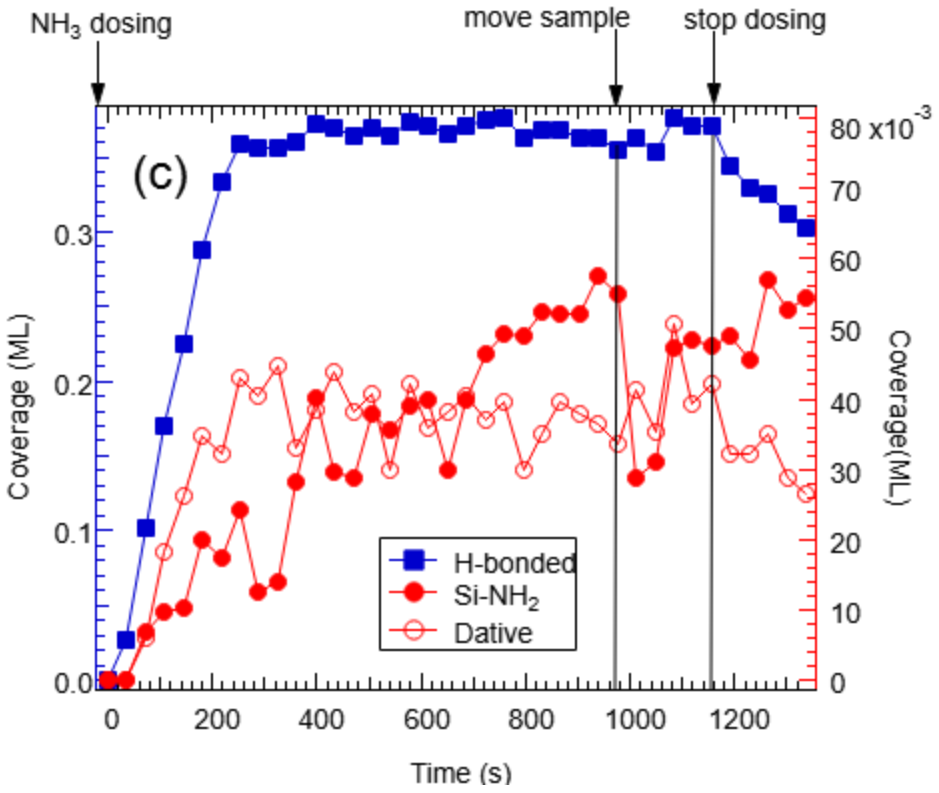
NH3 dosing
move sample
stop dosing
(c)
Coverage (ML)
Coverage(ML)
80 x10-3
70
60
50
40
30
20
10
0
0.3
0.2
0.1
0.0
0
200
400
600
800
1000
1200
Time (s)
H-bonded
Si-NH2
Dative

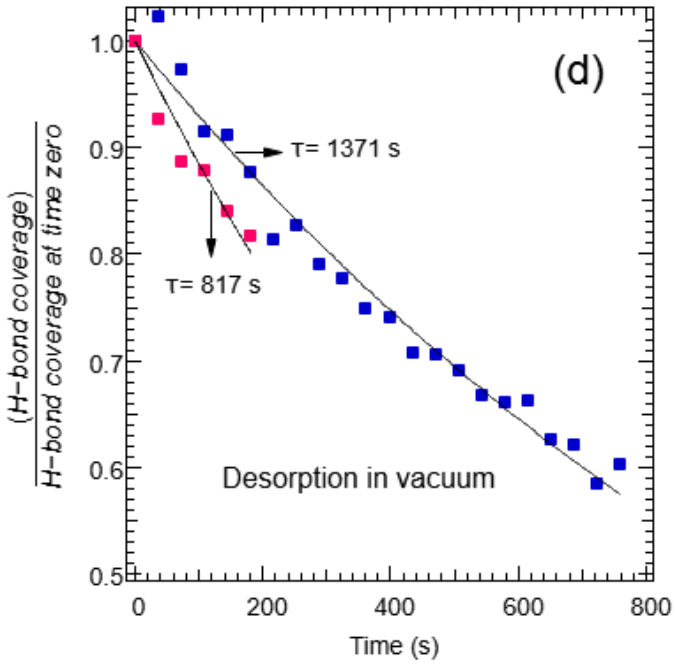
(d)
τ= 1371 s
τ= 817 s
Desorption in vacuum
(H-bond coverage) / H-bond coverage at time zero
1.0
0.9
0.8
0.7
0.6
0.5
0
200
400
600
800
Time (s)

Figure 4. (a) Time resolved N 1s spectra measured during NH_3 adsorption on (H,OH)-Si(001)-2×1 at 120 K (under 5 10^{-9} mbar of ammonia) with a photon energy of 455 eV (each spectrum shown here is the sum of 5 individual spectra). The baseline measured before NH_3 dosing was subtracted. All binding energies are aligned to a common position of the Si $2p_{3/2}$ core-level at 99.41 eV (the Si $2p_{3/2}$ binding energy of n^+ (H,OH)-Si(001) at room temperature). (b) Illustrative spectrum measured while dosing at t=180 s (Q= 0.5 ML) and corresponding fittings with three Gaussian components, datively bonded NH_3, H-bonded NH_3, and dissociated Si-NH_2 species. The full width at half maximum is 1.8 eV for all peaks, the binding energy is also indicated. (c) Nitrogen coverage (in ML) as a function of time for H-bonded NH_3, datively bonded NH_3 and dissociated Si-NH_2 species. (d) Desorption curves in vacuum plotted against time (time zero is the time at which the spectra start to be acquired). Coverages are divided by the value at time zero. The red square curve corresponds to desorption from a coverage of 0.37 ML, and the blue square one from a coverage estimated to be 0.25 ML. The curves are fitted by a decaying exponential ($\exp(-\frac{t}{\tau})$).

The N 1s spectrum in Figure 4(b) is recorded just before the onset of saturation. It is fitted with three components. The lowest binding energy component at 398.87 eV is attributed to dissociated ammonia Si-NH_2. We base our attribution on previous XPS studies on the adsorption of ammonia on clean Si(001)-2×1.[47,51] The highest binding energy component at 401.73 eV, + 2.86 eV above the $SiNH_2$ component, is attributed to ammonia datively bonded to a silicon dimer, as the predicted CLS_{per}^{th} and ΔIE_{QC}^{th} values (Tables 1 and 2) are both equal to 3.0 eV.

The third (middle) component found at 400.53 eV, is shifted by +1.66 eV with respect to the Si-NH_2 component. Looking to the periodic (cluster QC) DFT values in Table 1 (Table 2), we see that the NH_3(A,D) and NH_3(A,d) configurations have CLS_{per}^{th} (ΔIE_{QC}^{th}) values in the 1.41-1.51 eV range (1.5-1.7 eV range). Therefore, the main central component is attributed to ammonia making acceptor/donor bonds with *two* hydroxyls. The formation of purely acceptor configurations is excluded because the theoretical chemical shifts with respect to $SiNH_2$ (2.2 eV in periodic DFT, and 2.3±0.2 eV in cluster QC DFT) are much larger than the experimental ~1.6 eV shift.

The presence of acceptor-donor geometries is explained simply by the binding strength of the molecule on the surface. The $-E_{ads}$ values in Table 1 show that the SP-NH_3(A,D) and the CBP-NH_3(A,d) geometries (Figure 2) correspond to ammonia molecules that are the most firmly bound to the hydroxyls. Indeed, the $-E_{ads}$ value of the SP-NH_3(A,A) geometry is 0.3 eV lower. Neither single nor double donor geometries enter into consideration, as their $-E_{ads}$ values are much too low (0.06-0.18 eV), making them unobservable at 130 K.

In section S3 of SI, we give a detailed theoretical account of the effect of H-bond formation on the O 1s IE_{QC}^{th} of the hydroxyls, and discuss the O 1s ΔIE_{QC}^{th} taking the isolated SiOH as a reference. In section S4 we show the modifications of the O 1s after ammonia adsorption at 130 K. The experimental O 1s spectrum is significantly broadened and shifted to lower binding energy with respect to that of the pristine (H,OH)-Si(001) surface at 300 K, where the effects of H-bonding are supposed to be negligible. Theory explains qualitatively the experimental shift to lower binding energy, because the donor bond, OH(D) leads to a negative variation in ΔIE_{QC}^{th} significantly greater in magnitude than that of the acceptor bond, OH(A or a), which is positive.

Adsorption Kinetics of H-bonded ammonia and saturation coverage.

Figure 4(c) shows that the rate of adsorption of H-bonded ammonia, NH_3(A,D) or NH_3(A,d), is constant (1.52×10^{-3} ML s^{-1}) up to 216 s (Q=0.59 ML), corresponding to an initial sticking coefficient of 0.6. Above that critical dose, the rate goes to zero and the maximum coverage reached is 0.36 ML. This kinetic behavior suggests the presence of a molecular precursor.[52] The saturation coverage is larger than 0.25 ML, the value expected for a configuration in which one ammonia is bonded to two OHs and each OH to only one ammonia. Some OHs are necessarily bonded to two ammonia molecules. Ammonia and OHs likely forms strings of the type: …NH_3…OH…NH_3… where OHs are both donor and acceptor (see also SI, section S3 and S4).

We note also that the maximum coverage of H-bonded ammonia is not affected by synchrotron beam damage (see below for the other species): when a fresh area is probed by moving the sample the H-bonded coverage remains the same.

Desorption Kinetics at 130 K

As shown in Figure 4(c), once ammonia dosing is stopped (after 1150 s), the vessel is pumped down. We see that the H-bonded ammonia coverage starts to decrease. Assuming a first order reaction, the normalized coverage will be proportional to $\exp(-\frac{t}{\tau})$, where τ is the time constant. We find $\tau = 817$ s for an initial coverage of 0.37 ML (red squares in panel(d)) This experience has been repeated from a coverage of about 0.25 ML (blue squares in panel (d)) and we have found a characteristic time τ of 1371 s. A Gibbs energy of activation $\Delta G^{\ddagger}$ in the range 0.39-0.40

eV is obtained, using the Eyring-Polanyi-Evans equation valid for unimolecular desorption (the transmission coefficient is assumed to be one):

$$\tau^{-1} = \frac{k_B T}{h} \exp(-\frac{\Delta G^{\ddagger}}{k_B T})$$

where k_B is the Boltzmann constant and h the Planck constant ($k_B T/h$ is 2.7×10^{12} s^{-1} at 130 K). Assuming that adsorption is barrierless, $\Delta G^{\ddagger} = -\Delta G_{ads} = -(\Delta H_{ads} - T\Delta S_{ads})$. The increase of τ when the starting coverage is lower may indicate that the magnitude of ΔG_{ads} increases when the adsorption sites are less crowded. We recall that the calculated $-E_{ads}(= -\Delta H_{ads})$ values are in the range 0.56-0.69 eV (with PBE calculation errors of the order of 0.1 eV) for dual H-bonded geometries.

Probing the silicon dangling bonds with datively bonded ammonia

The adsorption kinetics of the dative species (component at 402 eV) is shown in Figure 4(c). We observe an initial linear regime up to 216 s (Q=0.59 ML), with an adsorption rate of 2.06×10^{-4} ML s^{-1}, corresponding to a sticking coefficient of 0.075, one order of magnitude smaller than that of the H-bonded species. Then a maximum coverage 4.4×10^{-2} ML is reached at 400 s (Q= 1 ML), after which the surface density of Si-NH_3 tends to decrease. This decrease is due, in part (see below), to the exposure to the beam: when the beam spot is moved, we recover a coverage of 4.6×10^{-2} ML in the freshly analyzed area. Considering the observed maximum coverage of datively bonded species (also around 4×10^{-2} ML), most of the silicon dangling bond sites should be occupied by ammonia.

We emphasize that the dative bonding of other Lewis bases than ammonia on *n*+-doped (H,OH)-Si(001) is also observed. Trimethylamine (a tertiary amine) does bond this way at 130 K, as proven by its N 1s spectrum given in Figure S6, section S5 of the SI. The coverage is 0.03 ML, a value comparable to the surface density of IDBs. However, the observation of a datively bonded species on an isolated tri-coordinated silicon atom may seem surprising. Indeed, in a simple acid-base reaction scheme, the formation of a Lewis adduct requires that the base (ammonia or trimethylamine) inserts its nitrogen lone-pair into an acidic site (an empty, positively charged silicon dangling bond). For instance, this applies to the case of the buckled clean surface.[53,54] However, for an n^+ substrate, the dangling bond is doubly occupied, i.e. negatively charged.[18] Therefore, one would expect the ammonia to be repelled when it approaches the tri-coordinated silicon adsorption site. As a dative bonding is observed, this means that the electron charge on the silicon defect is delocalized into the substrate when the tri-coordinated silicon atom is attacked by the ammonia molecule. We recall that the adsorption of ammonia molecules and amines on *n*-type H-terminated Si(111) SOI induces a strong electron-accumulation layer.[38] Adsorption likely takes place at silicon dangling bonds on that surface. Indeed, calculations[39] addressed the electronic structure of NH_3 bonded to the isolated dangling bonds of the H-terminated $\sqrt{3} \times \sqrt{3}$ Si(111) surface (the latter one mimics mesoporous Si). It was shown first that the molecule is bonded to the surface with $-E_{ads}$=0.45 eV, and second, a shallow donor state appears just below the conduction band of silicon.

Dissociation

Figure 4(c) shows that the initial adsorption rate of the Si-NH_2 species is also approximately constant and equal to ~0.7×10^{-4} ML s^{-1}. The synchrotron beam has a clear effect on breaking the ammonia molecule. After moving the spot (at 865 s), the Si-NH_2 coverage diminishes from ~0.06 ML to ~0.03 ML. This coverage is not zero, therefore dissociation may also occur in the absence of the beam, but the exposure to the beam multiplies the rate by *at least* a factor of ~2.

We first consider a mechanism leading to the dissociation of a molecule datively bonded to an IDB into Si-NH_2 and Si-H moieties *without* the assistance of the beam. In the case of the clean dimerized surface,[51,54] two adjacent silicon dangling bonds (e.g. on the same dimer) are necessary. Such a situation is not encountered on (H,OH)-Si(001), as the IDBs, immobile at 130 K,[55] are too far apart (2 nm on the average for a coverage of 0.04 ML). The proton relay mechanism, that has a low activation barrier, could be a solution to the problem.[51,56,57] One could imagine that a string of H-bonded moieties (ammonia-hydroxyl-ammonia-hydroxyl…) connects the Si-NH_3 precursor to a distant second dangling bond. Once a proton leaves the ammonia molecule, another proton is transferred to the uncapped silicon atom far away.

Concerning ammonia dissociation due to the beam, the effect of light is indirect. In fact, electrons matter. Under X-ray irradiation photoelectrons and Auger electrons travelling in the silicon substrate suffer inelastic losses. Secondary electrons that have sufficient kinetic energies escape into the vacuum (the "tail" of the secondary electrons extends several eV above the vacuum level[58]) and then can interact with the adsorbates. For NH_3 in the gas phase, a dissociative attachment resonant state is observed at 5.5 eV[59] above the vacuum level. Attachment-dissociation can lead to the breaking of the adsorbed molecule into $NH_2^{\bullet}$ + H^- or

NH_2^- + H•. If a molecule datively bonded to an IDB breaks after attaching an electron, a Si-NH_2 moiety will form, and the leaving H will react further apart forming a new bond, e.g. abstracting another H from a Si-H, breaking a Si-Si bond etc.. For H-bonded or physisorbed molecules, the formation of a Si-NH_2 moiety may need two steps, as in the mechanism proposed by Guizot et al..[60] In a first instance, a radical (H• or NH_2•) abstracts one H from a surface hydride (regenerating a H_2 or an NH_3 molecule). This leaves a Si• which, in a second instance, captures another NH_2• radical. In any case, Si-NH_2 formation via a mechanism involving an NH_2• radical does not necessarily require the occurrence of two adjacent silicon dangling bonds.

4 Conclusion

Water-terminated Si(001)-2×1, which presents well-identified OH patterns, is the ideal surface to study molecular adsorption via H-bond formation both at experimental and theoretical levels. We show that real-time, in situ XPS and DFT calculations (Periodic DFT and Cluster Quantum Chemistry DFT) provide detailed information on the bonding configurations when they are used in combination. Periodic DFT was used to calculate adsorption energies E_{ads} and N 1s core-level binding energy shifts relative to dissociated ammonia ($SiNH_2$), while Quantum Chemistry DFT was adopted to calculate N 1s and O 1s ionization energies (IE_{QC}^{th}) using ad-hoc clusters describing the adsorption geometries. We find that the periodic DFT N 1s core-level binding energy shifts CLS_{per}^{th} and the cluster quantum chemistry N 1s ΔIE_{QC}^{th} are in excellent agreement, supporting of the validity of the approaches applied.

The theory-assisted interpretation of the N 1s spectra leads to the conclusion that each ammonia molecule sticks molecularly to the surface at 130 K, making one H-acceptor and one H-donor bonds with a pair of OHs. Under a pressure of 5×10^{-9} mbar, the maximum coverage achieved is ~0.35 ML. However, when ammonia is pumped down, the H-bonded ammonia coverage diminishes due to desorption. The estimated barrier energy for desorption is $\Delta G^{\ddagger}$~0.4 eV. This value can be compared to the "binding strength" $-E_{ads}$ of acceptor-donor geometries that are comprised between 0.56 eV and 0.69 eV, according to periodic DFT calculations ($\mathrm{at\ T} = 0$ K).

Besides the non-covalent, reversible attachments, XPS shows that about 4×10^{-2} monolayers of ammonia molecules are datively bonded to the silicon dangling bonds present on the surface. Molecular dissociation is also observed (Si-NH_2 fragments are detected by XPS), largely due to beam damage.

Until now, the (large) effects of H-bonding on nitrogen and oxygen 1s core-level binding energies have been insufficiently addressed in the XPS literature, probably because of the lack of theoretical support. We hope that the present work will stimulate further XPS studies, in contexts where H-bonding is of primary importance, from water/solid interfaces to supramolecular chemistry.

ASSOCIATED CONTENT

Supporting Information.

The following PDF format file "SupInfo_OH_ammonia" is available free of charge.

It contains additional XPS spectra, the methodology of N and O coverage calibration, and cluster QC DFT calculations of O 1s ionization energies relative to the surface hydroxyls that are compared to experimental data.

AUTHOR INFORMATION

Corresponding Authors

*E-mail :francois.rochet@sorbonne-universite.fr; jean-jacques.gallet@sorbonne-universite.fr

Author Contributions

The manuscript was written through contributions of all authors. All authors have given approval to the final version of the manuscript.

ACKNOWLEDGMENT

LPR thanks the Ecole Doctorale ED388 of Sorbonne Université for her PhD grant. We thank Dr Federico Iori (Air Liquide, France) for providing us with "ball-and-stick" simulations of the (H,OH)-Si(001) surface.

TOC Graphic

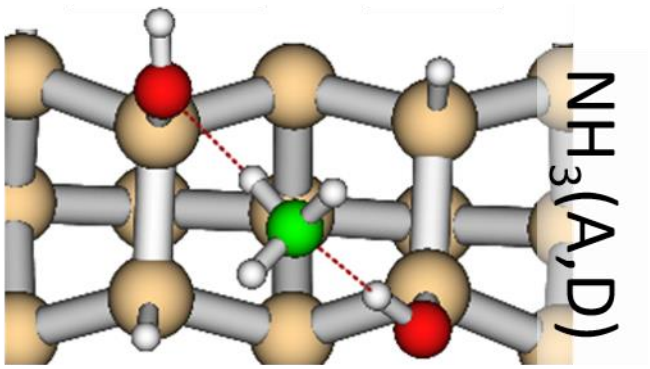
NH3(A,D)

REFERENCES

(1) Huggins, M. L. 50 Years of Hydrogen Bond Theory. *Angew. Chemie Int. Ed. English* **1971**, *10*, 147–152.

(2) Gilli, P.; Gilli, G. Noncovalent Interactions in Crystals. In *Supramolecular Chemistry*; John Wiley & Sons, Ltd: Chichester, UK, 2012.

(3) Zhang, H.; Zhou, P.; Chen, Z.; Song, W.; Ji, H.; Ma, W.; Chen, C.; Zhao, J. Hydrogen-Bond Bridged Water Oxidation on {001} Surfaces of Anatase TiO 2. *J. Phys. Chem. C* **2017**, *121*, 2251–2257.

(4) Kato, H. S.; Kawai, M.; Akagi, K.; Tsuneyuki, S. Interaction of Condensed Water Molecules with Hydroxyl and Hydrogen Groups on Si(001). *Surf. Sci.* **2005**, *587*, 34–40.

(5) De Renzi, V.; Lavagnino, L.; Corradini, V.; Biagi, R.; Canepa, M.; del Pennino, U. Very Low Energy Vibrational Modes as a Fingerprint of H-Bond Network Formation: L-Cysteine on Au(111). *J. Phys. Chem. C* **2008**, *112*, 14439–14445.

(6) George, I.; Viel, P.; Bureau, C.; Suski, J.; Lécayon, G. Study of the Silicon/γ-APS/Pyralin Assembly Interfaces by X-Ray Photoelectron Spectroscopy. *Surf. Interface Anal.* **1996**, *24*, 774–780.

(7) Kowalczyk, D.; Slomkowski, S.; Chehimi, M. M.; Delamar, M. Adsorption of Aminopropyltriethoxy Silane on Quartz: An XPS and Contact Angle Measurements Study. *Int. J. Adhes. Adhes.* **1996**, *16*, 227–232.

(8) Metwalli, E.; Haines, D.; Becker, O.; Conzone, S.; Pantano, C. G. Surface Characterizations of Mono-, Di-, and Tri-Aminosilane Treated Glass Substrates. *J. Colloid*

Interface Sci. **2006**, *298*, 825–831.

(9) Felicíssimo, V. C.; Minkov, I.; Guimarães, F. F.; Gel'mukhanov, F.; Cesar, A.; Ågren, H. A Theoretical Study of the Role of the Hydrogen Bond on Core Ionization of the Water Dimer. *Chem. Phys.* **2005**, *312*, 311–318.

(10) Carniato, S.; Gallet, J.-J.; Rochet, F.; Dufour, G.; Bournel, F.; Rangan, S.; Verdini, A.; Floreano, L. Characterization of Hydroxyl Groups on Water-Reacted Si(001)-2×1 Using Synchrotron Radiation O 1s Core-Level Spectroscopies and Core-Excited State Density-Functional Calculations. *Phys. Rev. B* **2007**, *76*, 085321.

(11) Garcia-Gil, S.; Arnau, A.; Garcia-Lekue, A. Exploring Large O 1s and N 1s Core Level Shifts Due to Intermolecular Hydrogen Bond Formation in Organic Molecules. *Surf. Sci.* **2013**, *613*, 102–107.

(12) Patrick, C. E.; Giustino, F. Structure of a Water Monolayer on the Anatase TiO2 (101) Surface. *Phys. Rev. Appl.* **2014**, *2*, 014001.

(13) Schaefer, A.; Lanzilotto, V.; Cappel, U.; Uvdal, P.; Borg, A.; Sandell, A. First Layer Water Phases on Anatase TiO2(101). *Surf. Sci.* **2018**, *674*, 25–31.

(14) Andersohn, L.; Köhler, U. In Situ Observation of Water Adsorption on Si(100) with Scanning Tunneling Microscopy. *Surf. Sci.* **1993**, *284*, 77–90.

(15) Poncey, C.; Rochet, F.; Dufour, G.; Roulet, H.; Sirotti, F.; Panaccione, G. Adsorption of Water on Si(001)-2 × 1 and Si(111)-7 × 7 Surfaces at 90 and 300 K: A Si 2p Core-Level and Valence Band Study with Synchrotron Radiation. *Surf. Sci.* **1995**, *338*, 143–156.

(16) Henderson, M. The Interaction of Water with Solid Surfaces: Fundamental Aspects

Revisited. *Surf. Sci. Rep.* **2002**, *46*, 1–308.

(17) Giustino, F.; Pasquarello, A. First-Principles Theory of Infrared Absorption Spectra at Surfaces and Interfaces: Application to the Si(100):H2O Surface. *Phys. Rev. B* **2008**, *78*, 075307.

(18) Gallet, J. J.; Bournel, F.; Rochet, F.; Köhler, U.; Kubsky, S.; Silly, M. G.; Sirotti, F.; Pierucci, D. Isolated Silicon Dangling Bonds on a Water-Saturated N+-Doped Si(001)-2 × 1 Surface: An XPS and STM Study. *J. Phys. Chem. C* **2011**, *115*, 7686–7693.

(19) Pierucci, D. The Electronic Structure and Reactivity of Tri-Coordinated Silicon Atoms on Water-Covered Si(001)Surface : Time-Resolved XPS and STM Studies, Université Pierre et Marie Curie, Paris, 2013.

(20) Skliar, D. B.; Willis, B. G. The Role of Dangling Bonds in H2O-Induced Oxidation of Si(100)-2 × 1. *J. Phys. Chem. C* **2008**, *112*, 9434–9442.

(21) Pierucci, D.; Gallet, J.-J.; Bournel, F.; Sirotti, F.; Silly, M. G.; Tissot, H.; Naitabdi, A.; Rochet, F. Real-Time X-Ray Photoemission Spectroscopy Study of Si(001)-2×1 Exposed to Water Vapor: Adsorption Kinetics, Fermi Level Positioning, and Electron Affinity Variations. *J. Phys. Chem. C* **2016**, *120*, 21631–21641.

(22) Willis, B. G.; Mathew, A.; Wielunski, L. S.; Opila, R. L. Adsorption and Reaction of HfCl4 with H2O-Terminated Si(100)-2 × 1. *J. Phys. Chem. C* **2008**, *112*, 1994–2003.

(23) Thissen, P.; Seitz, O.; Chabal, Y. J. Wet Chemical Surface Functionalization of Oxide-Free Silicon. *Prog. Surf. Sci.* **2012**, *87*, 272–290.

(24) McDonnell, S.; Longo, R. C.; Seitz, O.; Ballard, J. B.; Mordi, G.; Dick, D.; Owen, J. H.

G.; Randall, J. N.; Kim, J.; Chabal, Y. J.; Cho, K.; Wallace, R. M. Controlling the Atomic Layer Deposition of Titanium Dioxide on Silicon: Dependence on Surface Termination. *J. Phys. Chem. C* **2013**, *117*, 20250–20259.

(25) Longo, R. C.; Owen, J. H. G.; McDonnell, S.; Dick, D.; Ballard, J. B.; Randall, J. N.; Wallace, R. M.; Chabal, Y. J.; Cho, K. Toward Atomic-Scale Patterned Atomic Layer Deposition: Reactions of Al_2O_3 Precursors on a Si(001) Surface with Mixed Functionalizations. *J. Phys. Chem. C* **2016**, *120*, 2628–2641.

(26) Ihm, K.; Kang, T.-H.; Han, J. H.; Moon, S.; Hwang, C. C.; Kim, K.-J.; Hwang, H.-N.; Jeon, C.-H.; Kim, H.-D.; Kim, B.; Park, C.-Y. Hydroxyl Group-Induced Adsorptions of 4-Nitro Benzoic Acid on the Si(100) Surface. *J. Electron Spectros. Relat. Phenomena* **2005**, *144–147*, 397–400.

(27) Bournel, F.; Gallet, J.-J.; Köhler, U.; Ellakhmissi, B. B.; Kubsky, S.; Carniato, S.; Rochet, F. Propanoate Grafting on (H,OH)-Si(0 0 1)-2 × 1. *J. Phys. Condens. Matter* **2015**, *27*, 054005.

(28) Himpsel, F.; McFeely, F.; Taleb-Ibrahimi, A.; Yarmoff, J.; Hollinger, G. Microscopic Structure of the SiO_{2}/Si Interface. *Phys. Rev. B* **1988**, *38*, 6084–6096.

(29) Lee, S.-H.; Kang, M.-H. Dissociative Adsorption of Water on the Si(001) Surface: A First-Principles Study. *Phys. Rev. B* **2000**, *61*, 4503–4506.

(30) Lee, J.-Y.; Cho, J.-H. Two Dissociation Pathways of Water and Ammonia on the Si(001) Surface. *J. Phys. Chem. B* **2006**, *110*, 18455–18458.

(31) Yu, S.-Y.; Kim, Y.-S.; Kim, H.; Koo, J.-Y. Influence of Flipping Si Dimers on the

Dissociation Pathways of Water Molecules on Si(001). *J. Phys. Chem. C* **2011**, *115*, 24800–24803.

(32) Tielens, F.; Gervais, C.; Lambert, J. F.; Mauri, F.; Costa, D. Ab Initio Study of the Hydroxylated Surface of Amorphous Silica: A Representative Model. *Chem. Mater.* **2008**, *20*, 3336–3344.

(33) Klaus, J. W.; George, S. M. Atomic Layer Deposition of SiO2 at Room Temperature Using NH3-Catalyzed Sequential Surface Reactions. *Surf. Sci.* **2000**, *447*, 81–90.

(34) Ferguson, J. D.; Smith, E. R.; Weimer, a. W.; George, S. M. ALD of SiO2 at Room Temperature Using TEOS and H2O with NH3 as the Catalyst. *J. Electrochem. Soc.* **2004**, *151*, G528.

(35) Mayangsari, T. R.; Park, J.-M.; Yusup, L. L.; Gu, J.; Yoo, J.-H.; Kim, H.-D.; Lee, W.-J. Catalyzed Atomic Layer Deposition of Silicon Oxide at Ultralow Temperature Using Alkylamine. *Langmuir* **2018**, acs.langmuir.8b00147.

(36) Fang, G.; Chen, S.; Li, A.; Ma, J. Surface Pseudorotation in Lewis-Base-Catalyzed Atomic Layer Deposition of SiO 2 : Static Transition State Search and Born–Oppenheimer Molecular Dynamics Simulation. *J. Phys. Chem. C* **2012**, *116*, 26436–26448.

(37) Fang, G.; Xu, L.; Ma, J.; Li, A. Theoretical Understanding of the Reaction Mechanism of SiO 2 Atomic Layer Deposition. *Chem. Mater.* **2016**, *28*, 1247–1255.

(38) Dubey, G.; Rosei, F.; Lopinski, G. P. Molecular Modulation of Conductivity on H-Terminated Silicon-On-Insulator Substrates. *Small* **2010**, *6*, 2892–2899.

(39) Miranda-Durán, A.; Cartoixà, X.; Cruz Irisson, M.; Rurali, R. Molecular Doping and

Subsurface Dopant Reactivation in Si Nanowires. *Nano Lett.* **2010**, *10*, 3590–3595.

(40) Miranda, Á.; Cartoixà, X.; Canadell, E.; Rurali, R. NH3 Molecular Doping of Silicon Nanowires Grown along the [112], [110], [001], and [111] Orientations. *Nanoscale Res. Lett.* **2012**, *7*, 308.

(41) Pierucci, D.; Naitabdi, A.; Bournel, F.; Gallet, J.-J.; Tissot, H.; Carniato, S.; Rochet, F.; Köhler, U.; Laumann, D.; Kubsky, S.; Silly, M. G.; Sirotti, F. Benzaldehyde on Water-Saturated Si(001): Reaction with Isolated Silicon Dangling Bonds versus Concerted Hydrosilylation. *J. Phys. Chem. C* **2014**, *118*, 10005–10016.

(42) CPMD http://www.cpmd.org.

(43) Perdew, J. P.; Burke, K.; Ernzerhof, M. Generalized Gradient Approximation Made Simple. *Phys. Rev. Lett.* **1996**, *77*, 3865–3868.

(44) Car, R.; Parrinello, M. Unified Approach for Molecular Dynamics and Density-Functional Theory. *Phys. Rev. Lett.* **1985**, *55*, 2471–2474.

(45) Rignanese, G.-M.; Pasquarello, A.; Charlier, J.-C.; Gonze, X.; Car, R. Nitrogen Incorporation at Si(001)/SiO2 Interfaces: Relation between N 1s Core-Level Shifts and Microscopic Structure. *Phys. Rev. Lett.* **1997**, *79*, 5174–5177.

(46) Rignanese, G. M.; Pasquarello, A. First-Principles Study of NH3 Exposed Si(001)2×1: Relation between N 1s Core-Level Shifts and Atomic Structure. *Appl. Phys. Lett.* **2000**, *76*, 553–555.

(47) Mathieu, C.; Bai, X.; Bournel, F.; Gallet, J.-J.; Carniato, S.; Rochet, F.; Sirotti, F.; Silly, M. G.; Chauvet, C.; Krizmancic, D.; Hennies, F. Nitrogen 1s NEXAFS and XPS

Spectroscopy of NH3-Saturated Si(001)-2×1: Theoretical Predictions and Experimental Observations at 300 K. *Phys. Rev. B* **2009**, *79*, 205317.

(48) Gordon Group/GAMESS Homepage. Gordon Group/GAMESS Homepage http://www.msg.chem.iastate.edu/gamess/index.html (accessed Jun 7, 2013).

(49) Jolly, W. L.; Bomben, K. D.; Eyermann, C. J. Core-Electron Binding Energies for Gaseous Atoms and Molecules. *At. Data Nucl. Data Tables* **1984**, *31*, 433–493.

(50) Wandelt, K. The Local Work Function: Concept and Implications. *Appl. Surf. Sci.* **1997**, *111*, 1–10.

(51) Satta, M.; Flammini, R.; Goldoni, A.; Baraldi, A.; Lizzit, S.; Larciprete, R. Fundamental Role of the H-Bond Interaction in the Dissociation of NH3 on Si(001)-(2×1). *Phys. Rev. Lett.* **2012**, *109*, 036102.

(52) Lipponer, M. A.; Reutzel, M.; Dürr, M.; Höfer, U. Energy Dependent Sticking Coefficients of Trimethylamine on Si(001)—Influence of the Datively Bonded Intermediate State on the Adsorption Dynamics. *Surf. Sci.* **2016**.

(53) Hossain, M. Z.; Machida, S.-I.; Yamashita, Y.; Mukai, K.; Yoshinobu, J. Purely Site-Specific Chemisorption and Conformation of Trimethylamine on Si(100)c(4 x 2). *J. Am. Chem. Soc.* **2003**, *125*, 9252–9253.

(54) Naitabdi, A.; Bournel, F.; Gallet, J.-J.; Markovits, A.; Rochet, F.; Borensztein, Y.; Silly, M. G.; Sirotti, F. Triethylamine on Si(001)-(2 × 1) at 300 K: Molecular Adsorption and Site Configurations Leading to Dissociation. *J. Phys. Chem. C* **2012**, *116*, 16473–16486.

(55) Vittadini, A.; Selloni, A.; Casarin, M. Binding and DifFusion of Hydroxyl Radicals on

Si(100): A First-Principles Study. *Phys. Rev. B* **1995**, *52*, 5885–5889.

(56) Huang, X.; Tian, R.-Y.; Xiao-BaoYang; Zhao, Y.-J. Complexity of H-Bonding between Polar Molecules on Si(100)-2×1 and Ge(100)-2×1 Surfaces. *Surf. Sci.* **2016**, *651*, 187–194.

(57) Kato, H. S.; Akagi, K.; Tsuneyuki, S.; Kawai, M. Long-Range Proton Transport for the Water Reaction on Si(001): Study of Hydrogen-Bonded Systems with a Model Liquid−solid Interface. *J. Phys. Chem. C* **2008**, *112*, 12879–12886.

(58) Cazaux, J. Calculated Influence of Work Function on SE Escape Probability and Secondary Electron Emission Yield. *Appl. Surf. Sci.* **2010**, *257*, 1002–1009.

(59) Ram, N. B.; Krishnakumar, E. Dissociative Electron Attachment Resonances in Ammonia: A Velocity Slice Imaging Based Study. *J. Chem. Phys.* **2012**, *136*, 164308.

(60) Guizot, J.-L.; Alnot, P.; Wyczisk, F.; Perrin, J.; Allain, B. Kinetics of Deposition and Electrical Properties of Silicon Nitride Films Obtained by 185 Nm Photolysis of SiH 4 - NH 3 Mixtures. *Semicond. Sci. Technol.* **1991**, *6*, 582–589.